

**X-ray Kerr rotation and ellipticity spectra at the  $2p$  edges of Fe, Co, and Ni**

H.-Ch. Mertins

*University of Applied Sciences Münster, Stegerwaldstrasse 39, 48565 Steinfurt, Germany*S. Valencia, D. Abramssohn, A. Gaupp, and W. Gudat  
*BESSY, Albert-Einstein Strasse 15, D-12489 Berlin, Germany*

P. M. Oppeneer

*Leibniz-Institute of Solid State and Materials Research, P.O. Box 270016, D-01171 Dresden, Germany*  
(Received 24 July 2003; revised manuscript received 17 September 2003; published 12 February 2004)

We present resonantly enhanced longitudinal magneto-optical Kerr rotation and ellipticity spectra measured across the  $2p$  absorption edges of amorphous Fe, Co, and Ni. The Kerr spectra are acquired by a complete polarization analysis of linearly polarized synchrotron radiation upon reflection from the ferromagnetic films. We observe large Kerr rotation angles of up to  $\pm 24^\circ$ , more than two orders of magnitude larger than detected in the visible energy range. Spectral contributions stemming from atomic transitions could be separated from interference effects by simulations based on the optical constants, which have been determined through independent experiments. For grazing incidence, we show theoretically and experimentally that the longitudinal Kerr rotation and ellipticity spectra are related to transversal Kerr effect spectra and x-ray magnetic circular dichroism reflection spectra, respectively.

DOI: 10.1103/PhysRevB.69.064407

PACS number(s): 78.20.Ci, 78.20.Ls

**I. INTRODUCTION**

X-ray magneto-optical spectroscopies such as the x-ray magnetic circular dichroism (XMCD),<sup>1,2</sup> the Faraday effect,<sup>3,4</sup> the magnetic linear dichroism (XMLD),<sup>5</sup> and the x-ray Voigt effect<sup>6</sup> are cutting-edge research methods for the investigation of magnetic properties. These spectroscopic techniques enable, for example, element-selective investigations and imaging of magnetic domain structures<sup>7</sup> that are not possible with visible light. Magneto-x-ray spectroscopies are, as a consequence, highly suitable tools for the investigation of new and technologically important magnetic materials such as magneto-resistive, spin-valve, and exchange-biased materials.<sup>8</sup> Among the available spectroscopies resonant magnetic scattering and specular reflectometry of circularly and linearly polarized soft x rays<sup>9–13</sup> on single layers as well as on multilayers<sup>14–16</sup> have gained increasing importance since the resonantly enhanced cross sections at absorption edges lead to large magnetic responses which can exceed those observed in XMCD absorption experiments.<sup>9</sup> The large size of the dichroic effects observable in reflection over a wide range of incident angles, as well as their sensitivity to layer thickness and interface roughness, designates these spectroscopies to be appropriate for the study of element-specific magnetic depth profiles of magnetic films or multilayers.<sup>17</sup>

At present two reflection-type spectroscopies are mostly employed: the XMCD in reflection and the transversal magneto-optical Kerr effect (T-MOKE).<sup>9,18</sup> For T-MOKE the reflectance  $R_{T\pm}$  of linearly  $p$ -polarized light is measured for two inverted magnetization directions each transversal to the scattering plane. The magnetic signal is defined by the normalized difference  $A_T = (R_{T+} - R_{T-}) / (R_{T+} + R_{T-})$ . For the XMCD in reflection the magnetic signal is given by  $A_C = (R_{C+} - R_{C-}) / (R_{C+} + R_{C-})$ , where  $R_{C\pm}$  is the reflectance

of left-, right circularly polarized light, or, equivalently, two inverted magnetization directions with components parallel to the lights' wave vector of one helicity type.<sup>9</sup>

A practically uninvestigated magneto-optical phenomenon in the soft x-ray regime is the longitudinal magneto-optical Kerr effect (L-MOKE), which is quite distinct from T-MOKE. L-MOKE is characterized by the rotation of the polarization plane and the appearance of elliptical polarization when linearly polarized light is reflected from samples that have a magnetization component parallel or antiparallel to the propagation direction of the light. A longitudinal Kerr measurement requires a full polarization analysis of the light after its interaction with the material. The polarization analysis reveals information not only on the intensity, but additionally on the phase of the light.<sup>3,4,6</sup> With these data the real and imaginary part of the magneto-optical constant can completely be determined, something that is not possible with a single intensity measurement, such as T-MOKE or XMCD in reflection. In the visible range L-MOKE is a widely exploited standard technique for the characterization of magnetism and for microscopy of magnetic domains. While L-MOKE is small in the visible range, having typically rotation angles of the order of  $10^{-3}$  to  $10^{-1}$  degrees,<sup>19–21</sup> sizable effects are expected for the soft x-ray range due to the resonant enhancement occurring at the  $2p$  edges of  $3d$ -transition metals<sup>2,4</sup> or at the  $3d$  edges of rare-earth elements. In spite of this promising feature no experimental soft x-ray L-MOKE spectra exist, which is due to the lack of sensitive polarization detectors in this energy range. So far only one measurement of hysteresis loops at a fixed energy and fixed grazing incidence angle was reported that showed small Kerr rotation angles up to  $1.5^\circ$ .<sup>22</sup>

Here we present an experimental Kerr rotation and ellipticity spectra measured at the  $2p$  edges of Fe, Co, and Ni in L-MOKE geometry. We shall show that the Kerr spectra can

be described quantitatively by simulations using a macroscopic light-propagation formalism<sup>23</sup> and independently determined magneto-optical constants. This procedure allows the separation of contributions stemming from magneto-optical transitions and from interference effects. Furthermore, the relation between the L-MOKE spectra and simple intensity T-MOKE and XMCD spectra is shown by analytical expressions and confirmed experimentally.

## II. THEORY

To describe the longitudinal Kerr effect it is convenient to decompose the incident linearly polarized light into equal-amplitude left and right circularly polarized waves. The propagation of these waves in the material is governed by the complex magneto-optical constants  $n_{\pm} = 1 - (\delta_1 \pm \Delta\delta) + i(\beta_1 \pm \Delta\beta)$ , where the subscripts  $\pm$  refer to parallel/antiparallel orientation of photon helicity and sample magnetization. Here  $\delta_1$  and  $\beta_1$  account for the nonmagnetic dispersion and absorption, respectively, while  $\Delta\delta$  and  $\Delta\beta$  account for the respective magnetic contributions. The dichroic contribution can be expressed by the Voigt parameter  $Q$  which adopts for L-MOKE the form  $Q = (n_+ - n_-)/(n \sin \phi_i)$ , with  $n = 1/2(n_+ + n_-)$  and  $\phi_i$  is the complex angle of refraction measured with respect to the surface normal. Utilizing the Fresnel reflection coefficients  $r_{ss}$ ,  $r_{pp}$ , and  $r_{ps}$  for  $s$ - or  $p$ -polarized light, incident under the angle  $\phi_i$  the expression for the longitudinal Kerr effect can be derived:<sup>23</sup>

$$\theta_s + i\varepsilon_s = -r_{ps}/r_{ss} \approx \frac{-in_0nQ \cos \phi_i \tan \phi_t}{(n^2 - n_0^2) \cos(\phi_i - \phi_t)}, \quad (1a)$$

$$\theta_p + i\varepsilon_p = -r_{sp}/r_{pp} \approx \frac{-in_0nQ \cos \phi_i \tan \phi_t}{(n^2 - n_0^2) \cos(\phi_i + \phi_t)}, \quad (1b)$$

where  $\theta_{s,p}$  is the rotation over which the polarization plane is tilted and  $\varepsilon_{s,p}$  is the Kerr ellipticity. The indices stand for  $s$  or  $p$  geometry, respectively. The influence of the cap layer or of the vacuum enters by the index of refraction  $n_0$ . Since the optical contrast  $(n^2 - n_0^2)$  at the reflecting interface appears in the denominator, it can enlarge spectral structures, an effect that is not observed in absorption measurements.

The longitudinal Kerr data  $\theta$  and  $\varepsilon$ , that are obtained by polarization analysis, can be related to T-MOKE and reflection XMCD intensity-type measurements. We can use analytical expressions for T-MOKE and the XMCD in reflection<sup>9,23</sup> to derive the following relations between the different dichroic quantities for  $s$  and  $p$  geometries, respectively:

$$\begin{aligned} \theta_s &= A_T \operatorname{Re}\{\cos(\phi_i - \phi_t)/4 \cos \phi_i\} \\ &\approx A_T \operatorname{Re}\{n_0/4\sqrt{n^2 - n_0^2} + \cos \phi_i/4\}, \end{aligned} \quad (2a)$$

$$\begin{aligned} \theta_p &= A_T \operatorname{Re}\{\cos(\phi_i + \phi_t)/4 \cos \phi_i\} \\ &\approx A_T \operatorname{Re}\{n_0/4\sqrt{n^2 - n_0^2} - \cos \phi_i/4\}, \end{aligned} \quad (2b)$$

$$\varepsilon_s \approx \frac{1}{2}A_C + \cos \phi_i \operatorname{Im}\{r_{ps}\sqrt{n^2 - n_0^2}/n_0r_{ss}^2\}, \quad (3a)$$

$$\varepsilon_p \approx \frac{1}{2}A_C + \cos \phi_i \operatorname{Im}\{r_{sp}\sqrt{n^2 - n_0^2}/n_0r_{pp}^2\}. \quad (3b)$$

These are valid at grazing incidence where approximations for small angles are applied. The relations reveal that the Kerr rotation is proportional to the T-MOKE signal, which is obtained with an entirely different experimental technique. Analogously, the Kerr ellipticity can be related to the XMCD in reflection, which is obviously also measured in a different set-up as well as with circularly polarized light. These relations can be used to test the accuracy of L-MOKE spectra by comparing to T-MOKE and XMCD reflection spectra obtained from independent measurements.

## III. EXPERIMENT

The experiments were performed at the undulator beamlines U49-1-PGM and UE56-1-PGM-1 of BESSY.<sup>24</sup> The spectral resolution at the  $2p$  edges was roughly  $E/\Delta E = 2500$ . The degree of polarization was measured separately, giving  $P_{Lin} > 0.99$  for the L- and T-MOKE measurements and  $P_{Circ} = 0.9$  for the XMCD reflection measurements.<sup>24</sup> We used the BESSY ultra-high vacuum polarimeter chamber,<sup>25</sup> which allows experiments with variable angle of incidence from  $\phi_i = 90^\circ$  (grazing) to  $3^\circ$  (near normal incidence). Two magnetic coils supply variable magnetic fields between  $\pm 500$  Oe oriented in the sample's plane, either parallel (longitudinal) or perpendicular (transverse) to the plane of incidence.

The linear polarization of the incident or the reflected beam was analyzed by rotating a W/Si reflection multilayer (150 periods of 1.12-nm thickness each, angle of incidence set close to the Brewster angle) around the azimuthal angle  $\gamma$ , while the reflected intensity was monitored by a GaAs:P diode. The analyzer can be moved in to the reflected beam and aligned *in situ* which permits the polarization analysis to be performed at any angle of incidence. Alternatively, for intensity measurements the reflected intensity was monitored by moving a diode in to the beam. *In situ* exchange and removal of samples enables a quasismultaneously intensity or polarization analysis of the incident and of the reflected beam. The samples used for reflection experiments consisted of amorphous magnetron sputter deposited Fe, Co, or Ni layers of 30-nm thickness on Si wafers, capped with 3-nm Al to prevent oxidation.

## IV. RESULTS AND DISCUSSION

In the following we outline first the experimental procedure and analysis in some detail for the case of Co. Results for Fe and Ni are presented further below. In Fig. 1 the polarization measurements for Co are shown. The photon energy was set to 783 eV, just above the Co  $2p_{3/2}$  absorption edge where large effects are observed (see the inset). The normalized angular distribution of the incident beam as a function of the analyzer angle  $\gamma$  shows a maximum intensity

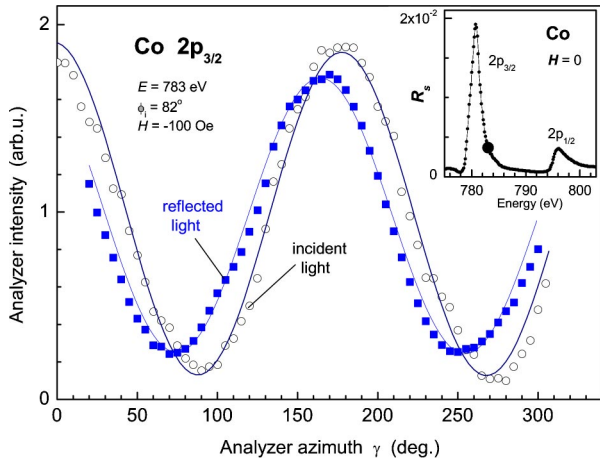


FIG. 1. (Color online) Measurement procedure for the x-ray longitudinal magneto-optical Kerr effect. The intensity of the light reflected from a Co sample (filled circles) at an energy close to the Co  $2p$  absorption edge (see inset) and that of incident light (open circles) are recorded. The continuous lines result from least square fits.

at  $\gamma=0^\circ$  and  $180^\circ$  corresponding to a horizontal polarization plane. Since the incident radiation is known to be completely linearly polarized<sup>24</sup> the analyzing power of the analyzer is found to be  $P_A = (R_s - R_p)/(R_s + R_p) = 0.87$ , deduced from reflectance measurements in  $s$ - or  $p$ -polarization geometry, respectively. After inserting the Co sample at grazing incidence, the polarization plane is rotated by  $\theta_s$ . The rotation angle and the ellipticity of the reflected light are obtained by a least-squares fit to the intensity  $I(\gamma) = I_R [1 + P_{Lin} P_A \cos 2(\gamma + \theta_s)]$ , with the fit parameters  $I_R$ ,  $P_{Lin}$  and  $\theta_s$ . Assuming fully polarized light the ellipticity is calculated from the degree of linear polarization  $P_{Lin}$ , applying  $\sin(2\varepsilon_s) = P_{Circ} = \sqrt{1 - P_{Lin}^2}$ .<sup>25</sup> After reflection, the circular polarization increases to  $P_{Circ} = 0.49$ , as shown by the decreased modulation depth of the analyzer spectrum. Several of such  $\gamma$  scans across the Co  $2p$  edge were taken to determine the Kerr rotation and ellipticity spectra, which are shown together with the reflectance in Fig. 2. The reflectance (top) is resonantly enhanced at the  $2p_{3/2}$  and  $2p_{1/2}$  edges. Below the  $2p_{3/2}$  edge, a minimum appears due to destructive interference of rays, reflected from the top surface and the interface between Co and the Si substrate. This interference structure is found to depend on the angle of incidence (not shown). The longitudinal Kerr rotation and ellipticity spectra are plotted in the middle and bottom panels, respectively. The measured x-ray Kerr rotation and ellipticity data are about two orders of magnitude larger than those observed for Co in the visible range.<sup>20</sup> A similar finding has been reported previously for soft x-ray Faraday experiments.<sup>3</sup> This enhancement of the x-ray magneto-optical effect is due to the strong spin-orbit coupling present for the  $2p$ - $3d$  excitations. We further note that our observed Kerr rotation values are one order of magnitude larger than the only one existing measurement, which showed rotations of up to  $1.5^\circ$ .<sup>22</sup>

The shape of the L-MOKE spectra can be analyzed to

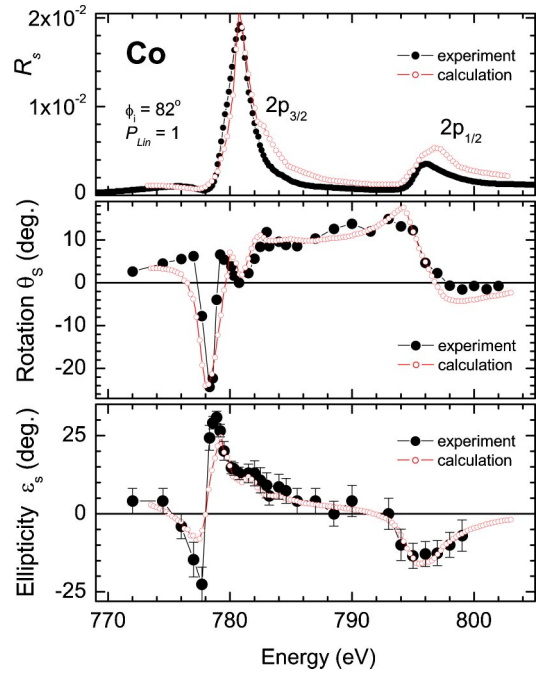


FIG. 2. (Color online) The reflectance and x-ray L-MOKE spectra measured at the  $2p$  absorption edge of an amorphous Co sample. Top: reflectance spectrum  $R_s$ . Middle: longitudinal x-ray Kerr rotation spectrum. Bottom: x-ray Kerr ellipticity spectrum. The filled points are experimental data, while the open points result from calculations utilizing independently determined optical and magneto-optical refractive indices (see Fig. 3). Error bars as indicated or smaller than the symbols.

result from the interplay of three individual contributions, which we discuss here for the Kerr rotation spectrum. These contributions are as follows. (1) The large Kerr rotation values of up to  $14^\circ$ , that are found right above the  $2p_{3/2}$  absorption edge and below the  $2p_{1/2}$  absorption edge, are induced by the magnetic contributions  $\Delta\delta$  and  $\Delta\beta$ , entering by the Voigt parameter  $Q$  [see Eq. (1)]. This is demonstrated with independently measured spectra of these magnetic parts of the refractive index (see Fig. 3, top). These  $\Delta\delta$  and  $\Delta\beta$  spectra were determined by resonant magnetic Bragg scattering of circularly polarized light from a Co/C multilayer ( $d = 4.1$  nm,  $P = 100$ ) employing a procedure described in Ref. 26. These data are confirmed by results from Faraday measurements on a 50-nm Co film according to a technique described in Ref. 3. (2) Between the  $2p$  edges the Kerr rotation displays a large maximum although the magnetic contributions  $\Delta\delta$  and  $\Delta\beta$  are small. Here the index of refraction  $n$  of the material as well as the optical constant  $n_0$  of the non-magnetic top layer comes into play. The spectral shape is dominated by the denominator  $(n^2 - n_0^2)$  [see Eq. (1)], which is close to zero between the  $2p$  edges. Indeed our experimentally determined refractive indices  $\beta_1$  and  $\delta_1$  of Co are close to  $\beta_0$  and  $\delta_0$  of the Al cap layer (see Fig. 3, bottom) as taken from tabulated values.<sup>27</sup> Such a large magneto-optical signal in between the edges is not observed in Faraday spectra, since the expression for the Faraday effect does not contain the denominator  $(n^2 - n_0^2)$ . A considerable enhancement of the x-ray polar Kerr rotation between the edges was recently

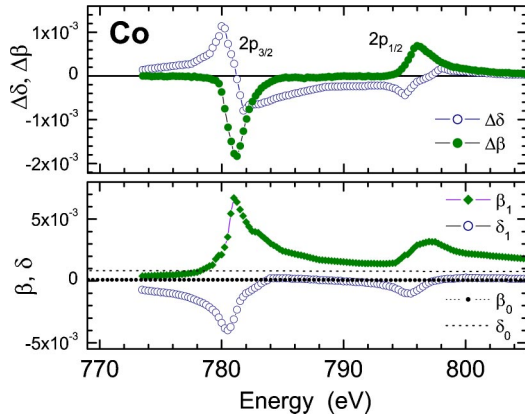


FIG. 3. (Color online) Optical and magneto-optical refractive indices determined across the Co  $2p$  edges by Faraday measurements and Bragg scattering. Top: the magnetic contributions  $\Delta\delta$  and  $\Delta\beta$  of Co. Bottom: the nonmagnetic refractive part  $\delta_1$  and the absorptive part  $\beta_1$  of Co. The refractive and absorptive parts  $\delta_0$  and  $\beta_0$  of the Al cap layer (Ref. 27) are shown by the dotted curves.

predicted by *ab initio* calculations,<sup>4</sup> which unambiguously identified the denominator to be the origin. (3) The singularity present at 778.5 eV is related to a third contribution. At this low energy no corresponding structure is found in the magneto-optical data  $\Delta\delta$  and  $\Delta\beta$  and neither in  $\beta_1$  and  $\delta_1$  (see Fig. 3). Also, the denominator ( $n^2 - n_0^2$ ) cannot account for this singularity. This sharp peak turns out to be an interference structure which is related to the interference minimum in the reflection spectrum at 778.5 eV. An inverse proportionality of the L-MOKE data and the reflectance spectrum follows from Eq. (1).

In order to achieve a quantitative description of the Kerr spectra we have to take into account all three above-mentioned contributions. We developed therefore a computer code, based on the formalism of Zak *et al.*<sup>28</sup> for magnetic layer systems. In Fig. 2 the results of these calculations are shown, which were computed using the experimentally determined optical constants plotted in Fig. 3. A quantitative agreement with the experimental L-MOKE spectra is obtained, even in the pre-edge region where interference effects are dominant. The reflectance  $R_s$  is reasonably reproduced. With this tool a separation of spectral features induced by magneto-optically active atomic transitions and structural-related interference effects is possible.

According to our theoretical considerations [Eqs. (2) and (3)] we expect a correlation between the longitudinal Kerr rotation and the T-MOKE signal and between the Kerr ellipticity and the XMCD reflection signal, respectively, for grazing incidence. Indeed, this is experimentally observed as shown in Fig. 4. The intensity data are scaled by the angular dependent prefactor. Both data sets show a good agreement in the energy region at and between the  $2p$  edges. However, differences appear in the pre-edge region for the T-MOKE spectra where the singularity due to interference is missing. Note, that Eqs. (2) and (3) do not take interference effects into account. The absence of the sharp peak in the T-MOKE spectrum is well understood—the average reflectance is can-

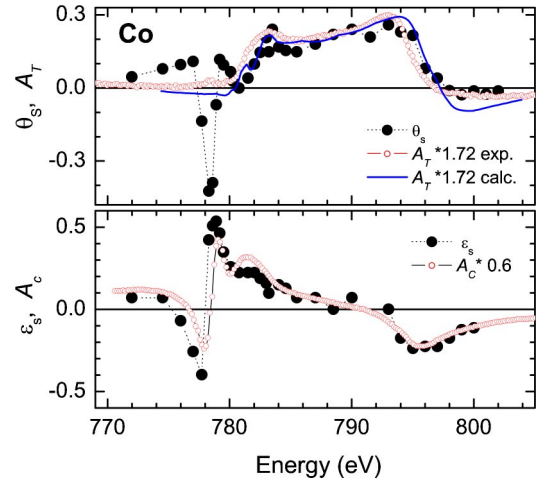


FIG. 4. (Color online) Comparison of x-ray L-MOKE spectra with spectra obtained from reflectivity measurements. Top: the longitudinal Kerr rotation and T-MOKE spectra across the Co  $2p$  edges. Bottom: the Kerr ellipticity and XMCD reflection spectra.

celled out by the normalization according to the definition. This is also confirmed by our simulations, based on the optical constants. The similarity of the longitudinal Kerr rotation and T-MOKE as well as that of the Kerr ellipticity and XMCD in reflection assure the accuracy of the measured x-ray L-MOKE spectra. For grazing incidence the technically more involved polarization measurement of the Kerr ellipticity can be substituted by the simpler XMCD intensity measurements, something that can be of practical importance. The Kerr rotation is related to the T-MOKE spectrum, however, the proportionality factor contains both  $n$  and  $n_0$ , which may introduce an energy dependence of the pre-factor.

The results for Fe (see Fig. 5) are comparable to those of Co. A similarity is observed for the reflectance as well as for

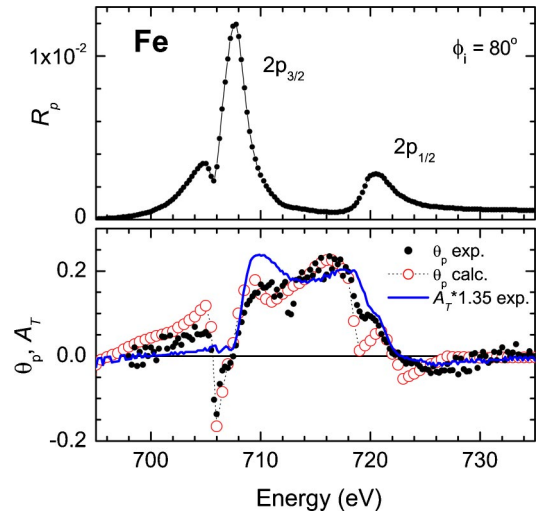


FIG. 5. (Color online) Top: reflectance across the Fe  $2p$  edge. Bottom: comparison of x-ray L-MOKE rotation spectra with T-MOKE spectra obtained from reflectivity measurements. The filled points are experimental data, while the open points result from calculations utilizing independently determined optical and magneto-optical refractive indices (Ref. 26).

the Kerr rotation. Both spectra are influenced by interference which leads to a minimum in the reflectance accompanied by an enhancement of the Kerr rotation near 706 eV. The agreement of the T-MOKE spectrum, scaled with the angular dependent prefactor, and the Kerr rotation spectrum is observed also for Fe except near 706 eV. This spectral discrepancy is explained by interference effects as discussed in detail above for Co. We confirm this explanation by simulations using our computer code. The used optical constants across the Fe  $2p$  edge have been determined independently and are presented in detail in Ref. 26. Note that the Fe Kerr spectra have been measured in  $p$ -geometry. According to Eq. (1) a spectral dependence similar to that obtained in  $s$ -geometry is expected for grazing incidence but with decreasing incidence angle towards normal incidence the Kerr data will differ. For  $p$ -polarized light a singularity (i.e., a  $\pm 90^\circ$  Kerr rotation) at the Brewster angle near  $45^\circ$  is expected while a smooth angular dependence is predicted for  $s$ -polarized light. The experimental observation of this feature needs a polarization analysis over the full angular range which is not yet feasible. Since the reflectance decreases nearly exponentially with the incidence angle sufficiently large signals could be recorded only from  $90^\circ$  down to  $80^\circ$ . Thus, for future experiments the sensitivity of the polarization analyzer has to be improved.

The results for Ni measured at an angle of incidence of  $83^\circ$  (see Fig. 6). The top panel shows the reflection spectra for two inverted transverse magnetization directions which are used for the determination of the T-MOKE signal. No interference minimum below the absorption edge is found. However a large reflectance peak is observed at the  $2p_{3/2}$  edge which may also be increased by positive interference. The Kerr spectra have been recorded only near the Ni  $2p_{3/2}$  edge, where a sufficiently high reflectance occurs. Above the edge the reflectance is considerably decreased. The polarization analysis could not be carried through above 864 eV with sufficient accuracy for such low intensity. The Kerr rotation data differ considerably from that of Co and Fe. In particular the pre-edge singularity is missing in the Kerr rotation spectrum of Ni. This is well understood and can be explained by the missing interference minimum in the reflectance spectrum. That this feature is not an artifact and that the L-MOKE spectrum is trustworthy, is exemplified by the corresponding T-MOKE spectrum. A simulation of the Ni spectra is not yet possible since the full set of optical constants across the Ni  $2p$  edge is not available.

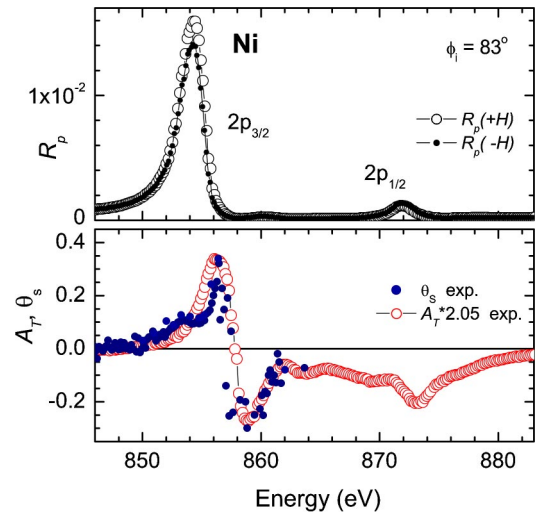


FIG. 6. (Color online) Top: reflectance across the Ni  $2p$  edge for two inverted transverse magnetization directions. Bottom: comparison of the x-ray L-MOKE rotation spectrum with T-MOKE spectrum obtained from reflectivity measurements.

## V. CONCLUSION

Experimental longitudinal Kerr spectra measured at the  $2p$  absorption edges of Co, Fe, and Ni are presented, showing large values at and in between the respective edges. Spectral contributions stemming from atomic transitions could be separated from interference effects by numerical simulations based on a macroscopic light-propagation formalism, and using optical constants, which were determined through independent experiments. Both experimentally and theoretically we showed that at grazing incidence the longitudinal Kerr spectra are related to T-MOKE and reflection XMCD spectra, obtained from simple reflectivity measurements. These relations could be helpful if a polarization analysis of the reflected beam is not possible. These features may be exploited for an element selective L-MOKE based microscopy of magnetic domains with synchrotron radiation.

## ACKNOWLEDGMENTS

The samples were prepared by O. Zaharko and H. Grimmer, PSI-Villigen. The polarization detector has been designed by T. Noll, BESSY and the project was financed by the German Federal Ministry for Education and Science (BMBF, No. 05KS1IPB/8).

<sup>1</sup>C. T. Chen, Y. U. Idzerda, H.-J. Lin, N. V. Smith, G. Meigs, E. Chaban, G. H. Ho, E. Pellegrin, and F. Sette, Phys. Rev. Lett. **75**, 152 (1995).

<sup>2</sup>J. B. Kortright and S. K. Kim, Phys. Rev. B **62**, 12 216 (2000).

<sup>3</sup>H.-Ch. Mertins, F. Schäfers, X. Le Cann, A. Gaupp, and W. Gudat, Phys. Rev. B **61**, R874 (2000).

<sup>4</sup>J. Kunes, P. M. Oppeneer, H.-Ch. Mertins, F. Schäfers, A. Gaupp, W. Gudat, and P. Novak, Phys. Rev. B **64**, 174417 (2001).

<sup>5</sup>S. S. Dhesi, G. van der Laan, E. Dudzik, and A. B. Shick, Phys. Rev. Lett. **87**, 077201 (2001).

<sup>6</sup>H.-Ch. Mertins, P. M. Oppeneer, J. Kunes, A. Gaupp, D. Abramsohn, and F. Schäfers, Phys. Rev. Lett. **87**, 047401 (2001).

<sup>7</sup>F. Nolting, A. Scholl, J. Stöhr, J. W. Seo, J. Fompeyrine, H. Siegwart, J.-P. Locquet, S. Anders, J. Lüning, E. E. Fullerton, M. F. Toney, M. R. Scheinfein, and H. A. Padmore, Nature (London) **405**, 767 (2000).

- <sup>8</sup>G. A. Prinz, *Science* **282**, 1660 (1998).
- <sup>9</sup>H.-Ch. Mertins, D. Abramssohn, A. Gaupp, F. Schäfers, W. Gudat, O. Zaharko, H. Grimmer, and P. M. Oppeneer, *Phys. Rev. B* **66**, 184404 (2002).
- <sup>10</sup>J. Geissler, E. Goering, M. Justen, F. Weigand, G. Schütz, J. Langer, D. Schmitz, H. Maletta, and R. Mattheis, *Phys. Rev. B* **65**, 020405 (2001).
- <sup>11</sup>L. Seve, N. Jaouen, J. M. Tonnerre, D. Raoux, F. Bartolome, M. Arend, W. Felsch, A. Rogalev, J. Goulon, C. Gautier, and J. F. Berar, *Phys. Rev. B* **60**, 9662 (1999).
- <sup>12</sup>P. M. Oppeneer, H.-Ch. Mertins, D. Abramssohn, A. Gaupp, W. Gudat, J. Kunes, and C. M. Schneider, *Phys. Rev. B* **67**, 052401 (2003).
- <sup>13</sup>O. Zaharko, P. M. Oppeneer, H. Grimmer, M. Horisberger, H.-Ch. Mertins, D. Abramssohn, F. Schäfers, A. Bill, and H.-B. Braun, *Phys. Rev. B* **66**, 134406 (2002).
- <sup>14</sup>L. Seve, J. M. Tonnerre, D. Raoux, *J. Appl. Crystallogr.* **31**, 700 (1998).
- <sup>15</sup>M. Sacchi, C. F. Hague, *Surf. Rev. Lett.* **9**, 811 (2002).
- <sup>16</sup>M. Sacchi, C. F. Hague, L. Pasquali, A. Mirone, J.-M. Mariot, P. Isberg, E. M. Gullikson, J. H. Underwood, *Phys. Rev. Lett.* **81**, 1521 (1998).
- <sup>17</sup>A. Kazimirov, J. Zegenhagen, and M. Cardona, *Science* **282**, 930 (1998).
- <sup>18</sup>C. C. Kao, J. B. Hastings, E. D. Johnson, D. P. Siddons, G. C. Smith, and G. A. Prinz, *Phys. Rev. Lett.* **65**, 373 (1990).
- <sup>19</sup>C. Robinson, *J. Opt. Soc. Am.* **53**, 681 (1963).
- <sup>20</sup>J. M. Ballantyne, *Phys. Rev. B* **54**, 1352 (1964).
- <sup>21</sup>S. Visnovsky, R. Krishnan, M. Nyvlt, V. Prosser, *J. Magn. Soc. Jpn.* **20**, S1, 41 (1996).
- <sup>22</sup>J. B. Kortright, D. D. Awschalom, J. Stöhr, S. D. Bader, Y. U. Idzerda, S. S. P. Parkin, I. K. Schuller, and H.-C. Siegmann, *J. Magn. Mater.* **207**, 7 (1999).
- <sup>23</sup>P. M. Oppeneer, in *Handbook of Magnetic Materials*, edited by K. H. J. Buschow (Elsevier, Amsterdam, 2001), Vol. 13, pp. 229–422.
- <sup>24</sup>M. R. Weiss, R. Follath, K. J. S. Sahwney, F. Senf, J. Bahrtdt, W. Frentrup, A. Gaupp, S. Sasaki, M. Scheer, H.-Ch. Mertins, D. Abramssohn, F. Schäfers, W. Kuch, and W. Mahler, *Nucl. Instrum. Methods Phys. Res. A* **467-8**, 449 (2001).
- <sup>25</sup>F. Schäfers, H.-Ch. Mertins, A. Gaupp, W. Gudat, M. Mertin, I. Packe, F. Schmolla, S. Di Fonzo, G. Soullié, W. Jark, R. Walker, X. Le Cann, M. Eriksson, and R. Nyholm, *Appl. Opt.* **38**, 4074 (1999).
- <sup>26</sup>H.-Ch. Mertins, O. Zaharko, A. Gaupp, F. Schäfers, D. Abramssohn, and H. Grimmer, *J. Magn. Mater.* **240**, 451 (2002).
- <sup>27</sup>L. Henke, E. Gullikson, and J. C. Davis, [http://www-cxro.lbl.gov/optical\\_constants/asf.html](http://www-cxro.lbl.gov/optical_constants/asf.html)
- <sup>28</sup>J. Zak, E. R. Moog, C. Liu, and S. D. Bader, *Phys. Rev. B* **43**, 6423 (1991).